

FULL TITLE
*ASP Conference Series, Vol. **VOLUME***, **YEAR OF PUBLICATION**
 NAMES OF EDITORS

Radio emission from WR140

S.M. Dougherty

National Research Council, D.R.A.O, P.O. Box 248, Penticton, BC, Canada

A.J. Beasley

*NRAO-AUI (ALMA), Camino del Observatorio 1515,
 Las Condes, Santiago, Chile*

M.J. Claussen

NRAO, 1003 Lopezville Rd., Socorro NM 87801, USA

B.A. Zauderer

*Department of Astronomy, University of Maryland,
 College Park, MD 20742, USA*

N.J. Bolingbroke

*Department of Physics and Astronomy, University of Victoria,
 3800 Finnerty Rd, Victoria, BC, Canada*

Abstract. Milliarcsecond resolution Very Long Baseline Array (VLBA) observations of the archetype WR+O star colliding-wind binary (CWB) system WR 140 have been obtained at 23 epochs between orbital phases 0.74 to 0.97. The emission in the wind-collision region (WCR) is resolved as a bow-shaped arc which rotates as the orbital phase progresses. This rotation provides for the first time the inclination of the orbit ($122^\circ \pm 5^\circ$), the longitude of the ascending node ($353^\circ \pm 3^\circ$), and the orbit semi-major axis (9.0 ± 0.5 mas). The implied distance is 1.85 ± 0.16 kpc, which requires the O star to be a supergiant, and leads to a wind-momentum ratio of 0.22. Quasi-simultaneous Very Large Array (VLA) observations show the synchrotron spectra evolve dramatically through the orbital phases observed, exhibiting both optically thin and optically thick emission. The optically thin emission maintains a spectral index of -0.5 , as expected from diffusive shock acceleration.

The archetype of CWB systems is the 7.9-year period WR+O system WR 140 (HD 193793). Its highly eccentric orbit ($e \approx 0.88$) modulates the dramatic variations in the emission from the system observed at many wavelengths. At radio wavelengths there is a slow rise from a low thermal state close to periastron of a few mJy, to a frequency-dependent peak in emission of 10's of mJy between orbital phase 0.65 to 0.85, before a precipitous decline just before periastron. The radio variations have been widely attributed to an underlying synchrotron source viewed through the changing free-free opacity of the extended stellar winds of the binary system along the line-of-sight to the WCR as the orbit progresses (Williams et al. 1990; White & Becker 1995). However, none of the free-free opacity models explain the radio light curve in a satisfactory manner. Models that include processes intrinsic to the WCR are now being explored (Pittard et al., in preparation).

We report briefly on high resolution observations of WR 140 obtained with the VLBA that image structures in the WCR at a linear resolution of a few AU, approximately the stellar separation at periastron, along with quasi-simultaneous VLA observations. Dougherty et al. (2004) include a more detailed description of this work.

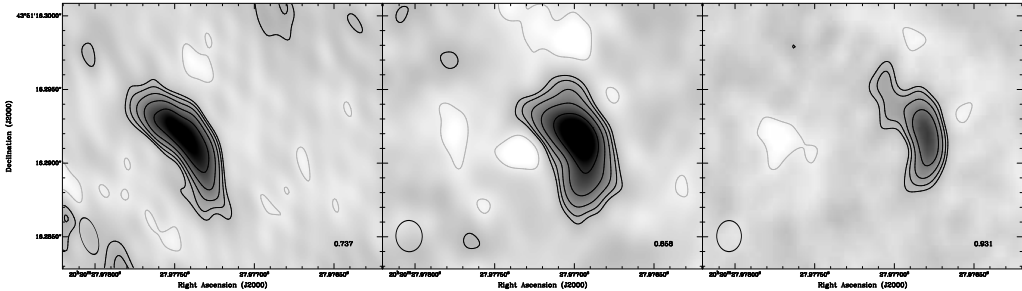


Figure 1. 8.4-GHz VLBA observations of WR140 at orbital phases 0.74, 0.86 and 0.93. The contour levels are $-1, 1, 1.6, 2.6, 4.1, 6.6, 10.5\rho$ where $\rho = 220 \text{ Jy beam}^{-1}$. The contour levels and greyscale are identical in each image. The beam size is shown in the lower left corner of the images, and is typically $2.0 \times 1.5 \text{ mas}^2$, which at a distance of 1.5 kpc gives a linear resolution of 3 AU. Rotation and proper motion of the WCR are clear.

1. Observations

Observations of WR 140 were obtained at 23 epochs using the VLBA. The campaign started on Jan 4, 1999 near the peak of radio emission around orbital phase 0.75 and was completed Nov 18, 2000 when the radio emission had declined to its low level. The resulting phase-referenced 8.4-GHz images at three of the observed epochs are shown in Fig. 1. Additionally, we also obtained closely concurrent observations with the VLA at five frequencies between 1.4 and 22 GHz.

The 8.4-GHz emission detected by the VLBA is clearly resolved. We identify this emission as arising from the WCR in WR 140 since this is the only emission in the system with sufficient brightness temperature ($> 10^5 \text{ K}$) to be detected by the VLBA. The stellar winds, with brightness of $\sim 10^4 \text{ K}$ are undetected. A bow-shaped ridge of emission is observed at most epochs, as anticipated for the WCR from model calculations (e.g. see Eichler & Usov 1993; Canto et al. 1996; Dougherty et al. 2003), with the bow shock wrapping around the star with the lower wind momentum - typically the O star. Between orbit phase 0.74 and 0.95, the WCR exhibits rotation from “pointing” NW to W, in addition to an east to west proper motion of $\sim 10 \text{ mas}$.

2. Orbital parameters of WR 140

Many of the orbital parameters in WR 140 are well-determined from radial velocity measurements (see Marchenko et al. 2003, and references therein). However, the orbital inclination (i), semi-major axis (a) and the longitude of the ascending node (Ω) can only be determined if the system can be resolved into a “visual” binary around the orbit. The two stellar components in WR 140 have been resolved using the Infrared-Optical Telescope Array (IOTA) interferometer on June 17, 2003 to have a separation of $12.9_{-0.4}^{+0.5} \text{ mas}$ at a position angle of $151.7_{-1.3}^{+1.8} \text{ degrees east of north}$ (Monnier et al. 2004). Assuming $P = 2899 \text{ days}$, $T_o = 2446147.4$, $e = 0.881$ and $\omega = 47^\circ$ (Marchenko et al. 2003), this single epoch observation at orbital phase 0.297 gives families of possible solutions for (i, Ω, a) .

Currently, the VLBA observations of the WCR are the only means to determine uniquely i , and hence Ω and a , from the possible IOTA solutions. Under the assumption that the free-free opacity along the line-of-sight to the WCR is sufficiently low as to not impact the apparent distribution of emission from the WCR, we expect the “arc” of WCR emission to wrap around the star with the lower wind momentum - the O star. In this case, the rotation of the WCR as the orbit progresses implies that O star moves from the SE to close to due E of the WR star over the period of the VLBA observations. Also, if it is assumed the axis of symmetry of the emission from the WCR is coincident

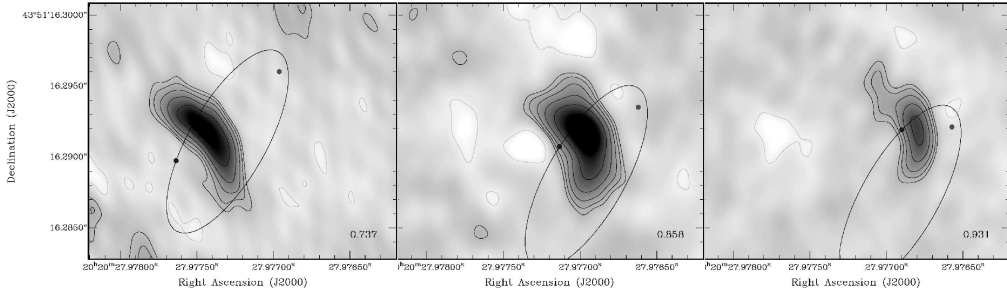


Figure 2. The derived orbit of WR 140 on the plane of the sky using $e = 0.88$, $\omega = 47^\circ$, $\Omega = 353^\circ$, $i = 122^\circ$ and $a = 9.0$ mas at orbital phase 0.737, 0.858 and 0.931, overlaid on the VLBA 8.4 GHz images. The WR star is to the W (right) of the WCR at these phases. The rotation of the WCR as the orbit progresses is clear. The relative position of the stars to the WCR was determined using a wind momentum ratio of 0.22 (see § 3.)

with the projection on the plane of the sky of the line-of-centres of the two stars, we can derive the orbital inclination from the change in the orientation of the WCR with orbital phase. Each (i, Ω) family provides a unique set of position angles for the projected line-of-centres as a function of orbital phase. By fitting the position angle of the line of symmetry of the WCR as a function of orbit phase for different sets of (i, Ω) , we find a best-fit solution of $i = 122^\circ \pm 5^\circ$ and $\Omega = 353^\circ \pm 3^\circ$. These values lead to a semi-major axis of $a = 9.0 \pm 0.5$ mas, and a projected orbit that evolves as shown in Fig. 2.

The derived orbit inclination is consistent with values previously suggested. However, it presents a challenge to current models of dust formation. To date, most models of dust formation in WR 140 assume that the gas from which dust is formed in the WCR is compressed within ~ 0.15 yr of periastron passage (Williams et al. 1990). The subsequent motion of the compressed gas is determined by the velocity of this material when it is compressed. Since the momentum of the WR star wind is higher than that of the O star, this material moves away from the WR star, along the WCR. With the orbit orientation derived here, the O star is NW of the WR star during periastron, and material compressed at periastron will therefore have a proper motion to the NW. However, high-resolution IR observations show that dust ejected during the 2001 periastron passage has proper motion to the south and east, away from the WR star (Monnier et al. 2002). New dust models are now attempting to address this challenge (Williams, this volume).

3. Basic system parameters of WR 140

Distance estimates of WR stars are typically based on absolute magnitude calibrations that often have large scatter. Having determined the orbital inclination and semi-major axis it is now possible to make an estimate of the distance to WR 140 *independent of any stellar parameters*. Marchenko et al. (2003) determined $a \sin i = 14.10 \pm 0.54$ AU, which leads to $a = 16.6 \pm 1.1$ AU for $i = 122^\circ \pm 5^\circ$. Along with the derived semi-major axis of $a = 9.0 \pm 0.5$ mas, these give a distance of 1.85 ± 0.16 kpc.

This distance is somewhat larger than the usually quoted value of 1.3 kpc deduced by Williams et al. (1990) from the luminosity of the system. Since the primary O-star luminosity indicator is masked by the WC7 spectrum, Williams et al. (1990) assumed a main sequence O4-5 star with an absolute magnitude of -5.6 and took that of the WC7 star to be -4.8 . With the system at 1.85 kpc, the absolute magnitude of the O4-5 star becomes -6.4 , suggesting it is a supergiant (see Vacca et al. 1996, Table 7).

Table 1. Basic parameters of WR 140

Parameter	Primary	Secondary	System
Distance (kpc)			1.85
M_v	-6.4	-5.6	-6.8
Spectral type	0.4-5 I ^a	WC7	
BC	-4.3 ^a	-3.4 ^b	
M_{bol}	-10.7	-9.0	
$\log(L_{bol}/L_\odot)$	6.18 ^c	5.5 ^c	
Mass (M_\odot)	54 ± 10	20 ± 4	
v_∞ (km s ⁻¹)	3100 ^d	2860 ^e	
\dot{M} (M_\odot yr ⁻¹)	8.7×10^{-6}	4.3×10^{-5}	

^aBased on M_v and the calibration of Vacca et al. (1996) ^bWilliams et al. (1990) ^cCalculated assuming $M_{\odot, bol} = 4.75^m$ (Allen 1976) ^dSetia Gunawan et al. (2001) ^eEenens & Williams (1994)

With the increase in distance, a reassessment of the mass-loss rates of the two stars is appropriate. Based on the X-ray luminosity measured by ASCA (Zhekov & Skinner 2000), the mass-loss rate for the WC star at 1.85 kpc is $4.3 \times 10^{-5} M_\odot$ yr⁻¹. Repolust et al. (2004) suggests values of $8.6 - 8.8 \times 10^{-6} M_\odot$ yr⁻¹ for O4-5 supergiants. Along with the wind speeds (Table 1) these mass-loss rates imply a wind momentum ratio $\eta = 0.22$. This wind-momentum ratio is considerably higher than the 0.035 deduced by Williams et al. (1990). The higher value of η derived here, however, implies a half-opening angle of the WCR of 63° (following Eichler & Usov (1993)), consistent with $65^\circ \pm 10^\circ$ derived from these VLBA observations.

4. The radio spectra of WR 140

The new VLA data at five frequencies allow us to observe the radio spectrum and its evolution better than previously possible, most particularly at the higher frequencies. At phase 0.974, the spectrum is a power-law with a spectral index of 0.72 ± 0.03 , a value characteristic of the stellar winds in WR+OB binary systems. Furthermore, the flux levels at this phase are consistent with the wind densities implied by the parameters in Table 1. Assuming the thermal emission from WR 140 is essentially constant throughout the orbit, the synchrotron spectra at each observed phase can be determined by simply subtracting the thermal flux at phase 0.974 from the total flux. The resulting spectra are shown in Fig. 3.

The synchrotron spectra between phases 0.67 and 0.92 are optically thin at several frequencies, with a spectral index that appears to be closely constant, with a slope of -0.5 ± 0.1 , as expected for diffusive shock acceleration of electrons in strong, non-relativistic shocks (e.g. Bell 1978; Drury 1983; Jones & Ellison 1991, and references therein). The optically thick spectrum apparent during the bulk of the orbit has been widely attributed to free-free absorption in the stellar winds along the line-of-sight to the WCR. Unfortunately, these models are too simple to explain the radio observations of WR 140, as readily acknowledged by their authors. The VLBA observations (Fig. 1) show the WCR as a distributed emission region and the lines-of-sight to the WCR traverse different regions of the stellar winds. As a result, the emerging emission will be a combination of both optically thick and thin emission since even though lines-of-sight to the apex may be optically thick, a substantial amount of emission arises from optically thin lines-of-sight to the downstream flow. Using the newly derived orbit and assuming a half-opening angle for the WCR of 63°, we now know the lines-of-sight to the WCR traverse the O-star wind between orbit phases 0.24 and 0.99 during which the most dramatic changes in the radio emission are observed. Clearly, if stellar wind free-free opacity plays any role in determining the observed spectra, it is the O-star wind opacity that is of most concern, not that of the WR star. Another shortcoming

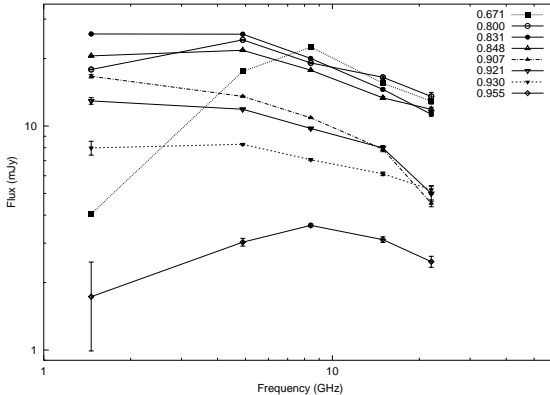


Figure 3. Synchrotron spectra of WR 140 at several orbital phases, determined by subtracting the thermal spectrum at phase 0.974 from the spectra at each phase. The key to the plot is shown in the upper right-hand corner.

of previous models is the assumption that synchrotron emission is optically thin at all observing frequencies, and at all orbital phases. The optically thick component of the spectra may, at least in part, be due to mechanisms intrinsic to the WCR.

New radiative transfer models, based on a fully consistent hydrodynamic treatment of the WCR, have started to explore the impact of a number of processes on the radio emission from CWBs, including free-free opacity in the stellar winds and the WCR, synchrotron self-absorption, Coulombic cooling through interactions with post-shock ions, plasma effects such as the Razin effect, and Inverse Compton cooling by the intense ultra-violet radiation field of the nearby massive stars. These models have been very successful in explaining the radio emission from very wide CWBs such as WR 147 (Dougherty et al. 2003), and are now maturing to the point where they will provide more insight to the mechanisms acting in WR 140 (Pittard et al., in preparation). The observations presented here represent the essential constraints for these new models.

References

Allen, C. W. 1976, *Astrophysical Quantities* (London: Athlone (3rd edition), 1976)
 Bell, A. R. 1978, MNRAS, 182, 147
 Canto, J., Raga, A. C., & Wilkin, F. P. 1996, ApJ, 469, 729
 Dougherty, S. M., Beasley, A. J., Claussen, M. J., Zauderer, B. A., & Bolingbroke, N. J. 2004, ApJ, submitted
 Dougherty, S. M., Pittard, J. M., Kasian, L., Coker, R. F., Williams, P. M., & Lloyd, H. M. 2003, A&A, 409, 217
 Drury, L. O. 1983, Reports of Progress in Physics, 46, 973
 Eenens, P. R. J. & Williams, P. M. 1994, MNRAS, 269, 1082
 Eichler, D. & Usov, V. 1993, ApJ, 402, 271
 Jones, F. C. & Ellison, D. C. 1991, Space Science Reviews, 58, 259
 Marchenko, S. V., Moffat, A. F. J., Ballereau, D. et al. 2003, ApJ, 596, 1295
 Monnier, J. D., Traub, W. A., Schloerb, F. P. et al. 2004, ApJ, 602, L57
 Monnier, J. D., Tuthill, P. G., & Danchi, W. C. 2002, ApJ, 567, L137
 Repolust, T., Puls, J., & Herrero, A. 2004, A&A, 415, 349
 Setia Gunawan, D. Y. A., van der Hucht, K. A., Williams, P. M., et al. 2001, A&A, 376, 460
 Vacca, W. D., Garmany, C. D., & Shull, J. M. 1996, ApJ, 460, 914
 White, R. L. & Becker, R. H. 1995, ApJ, 451, 352
 Williams, P. M., van der Hucht, K. A., Pollock, A. M. T., et al. 1990, MNRAS, 243, 662
 Zhekov, S. A. & Skinner, S. L. 2000, ApJ, 538, 808